MODELING ORIGAMI-LIKE STRUCTURES WITH NEAR ZERO STIFFNESS: MODAL ANALYSIS AND CREASE/WRINKLE CORRELATIONS

Antonio F. Avila

Fernanda L.R. Lima

Marina G. M. Martins

Guilherme C. Arantes

Matheus Norton

avila@ufmg.br

nandaalima12@gmail.com

marinageorgiam@gmail.com

garantesufmg@gmail.com

mtmelo11@hotmail.com

Universidade Federal de Minas Gerais, Department of Mechanical Engineering, 6627 Antonio Carlos Avenue, 31270-901, Belo Horizonte, MG. Brazil

Abstract. *This paper deals with near-zero thin membrane space structures based on origami configurations. Two different origami patterns were analyzed, i.e. Miura-Ori and Kresling. The first one largely employed for solar arrays in satellites and the second for space telescopes. To be able to correlate the crease/wrinkle effect with thin membranes, a series of tensile testes were employed. The origami-like structure natural frequencies were studied using modal analysis based on finite element. This analysis shows two new aspects on origami-like structures, i.e. the first one is the asymptotic behavior of natural frequencies with the increase on crease number for both Miura-Ori and Kresling origami-like structures. The second information is based on mode vibrations changes during the unfolding process, which it is also a critical during space structures deployment. The final feature is the fact that stiffness and strength are independent of the crease orientation for acetate membranes. Yet the non-linear stress-strain behavior is another issue to be taken into consideration for further analysis.*

Keywords: *Origami-like structures, Modal analysis, Crease/wrinkle effect on strength, shell element, near zero stiffness structures.*

INTRODUCTION

As described by Wang et al (2016), origami structures are widely applicable in fields such as self-folding machines, aerospace engineering, and bioengineering. As commented by Chen and Feng (2012), the reason for such versatility is the origami capability of undergo large configurations changes without cut or being stretched. The usage of origami techniques into space-structures, e.g. antennas, telescopes and solar panels, is a traditional approach employed for decades. These ultra-light space structures, in special Gossamer structures, are made of thin membranes made of polymeric composites with near zero stiffness. As described by Woo (2008), these thin membrane structures can have exceptionally light mass and packaged in a small volume. However, when these structures are under compressive loadings, buckling can occur very easily due to the almost non-existing bending stiffness. This local buckling can be seemed as wrinkles. According to Cai et al (2017), wrinkled regions can cause problems during the membranes' deployment. These problems can be identified as non-predicted angular and/or linear displacements, which can alter the membrane/panel final geometry. Papa and Pellegrino (2008) argued that wrinkles can also affect the membrane's stability and make the problem even worse. Wang et al (2011) discussed the wrinkle-crease effect into the overall structure/membrane design. For example, in the case of solar sails, creases/wrinkles can decrease the thrust forces and as explained by Papa and Pellegrino (2008) rise controllability issues. These problems, however, are not barriers for origami-like structures applications. The key issue is the unique overall properties of origami-like structures or origami-inspired materials.

According to Zhou et al (2016), origami-like structures or origami-inspired materials are man-made structures/materials that can be called metamaterials. These materials present unusual physical properties that arise mainly from the micro/macro-structure arrangement instead of the properties of constituents. Wei et al (2013) pointed out that origami-like structures are periodic. Therefore, it can be designed and analyzed based on the unit cell approach. This approach was employed by different researchers to be able to model the entire structure. Liu et al (2015) described a representative unit cell for the Miura-Ori origami folding pattern, which is one of the most used origami patterns into aerospace industry. According to Dutta and Graham (2017), a Miura-patterned foldable sheet (also called as Miura- Ori) is a two-dimensional tessellation of unit cells, each made up of four identical facets in the shape of parallelograms. The facets are assumed to be infinitely thin and rigid. When completely folded, all the facets of the sheet are co-planar, i.e. the sheet folds flat. Moreover, as discussed by Fang et al (2017), folding and unfolding of origami can be fast and reciprocal, and origami-based mechanical structure/metamaterials can be a medium for elastic wave propagation and vibration transmission. Therefore, a modal analysis on such structure/metamaterial is critical for a dynamic behavior understanding.

This paper investigates the natural frequencies and vibration modes of two different space structures, i.e. the first one is a two dimensional structure based on Miura-Ori folding pattern (largely employed for solar panel), while the second structure is a tube-like structure following the Kresling folding pattern (commonly employed for antennas and telescopes).

MODELING ORIGAMI-LIKE STRUCTURES

According to Yasuda and Yang (2015), Origami is defined as the handcrafted art of paper. Moreover, the folding process follows a repetitive pattern. This pattern defines an unit cell, which can be used to create a mathematical model of origami. Moreover, by defining some geometric parameters, i.e. angles and edge sizes, it is possible to make a parametrization of such unit cell. Therefore, by changing angles and edges' size, it is possible to simulate different stages during the folding/unfolding process. Liu et al (2015) proposed a parametrized unit cell which can be applied for Miura-Ori pattern from fully folded to fully deployed conditions. As discussed by Wei et l (2013), the Miura-Ori pattern can be represented by the unit cell shown in Figure 1. Moreover, this unit cell can mathematically be represented by two dihedral angles θ and β, both ranging from zero to pi, and one oblique angle α. In the unit cell *l* represents the length, while *w* and *h* are width and height, respectively.

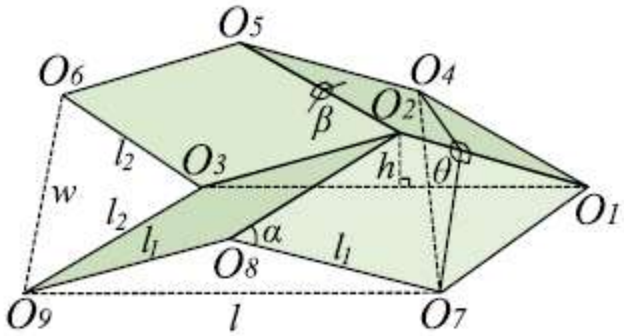

Figure 1. Miura-Ori Unit cell from Wei et al (2013)

The geometry of the unit cell can be defined by the following mathematical parameters:

$$\boldsymbol{\beta = 2sin^{-1}(\zeta sin(\theta/2))} \tag{1}$$

Proceedings of the XXXVIII Iberian Latin-American Congress on Computational Methods in Engineering
P.O. Faria, R.H. Lopez, L.F.F. Miguel, W.J.S. Gomes, M. Noronha (Editores), ABMEC, Florianópolis, SC, Brazil, November 5-8, 2017.

$$\boldsymbol{l = 2l_1\zeta} \quad (2)$$

$$\boldsymbol{w = 2l_2\xi} \quad (3)$$

$$\boldsymbol{h = l_1\zeta tan\alpha cos(\theta/2)} \quad (4)$$

Wei et al (2103) defined the dimensionless width and height as

$$\boldsymbol{\xi = sin\alpha sin(\theta/2)} \quad (5)$$

$$\boldsymbol{\zeta = cos\alpha(1-\xi^2)^{-1/2}} \quad (6)$$

From equations (1) through (6), it is possible to develop a close form set of equations to define each nodal coordinates into the Cartesian system. Table 1 summarizes each nodal component coordinates. Note that node 3 was selected as the origin.

Figure 2 represents the Miura-Ori origami following the equations described for the near fully folded (θ = 12 deg), and fully unfolded (θ ≈ 180 deg) for a constant oblique angle (α = 60 deg). The unit cell is reproduced 100 time (10 x10 mesh – on X-Y plane), with same edge size (50 mm).

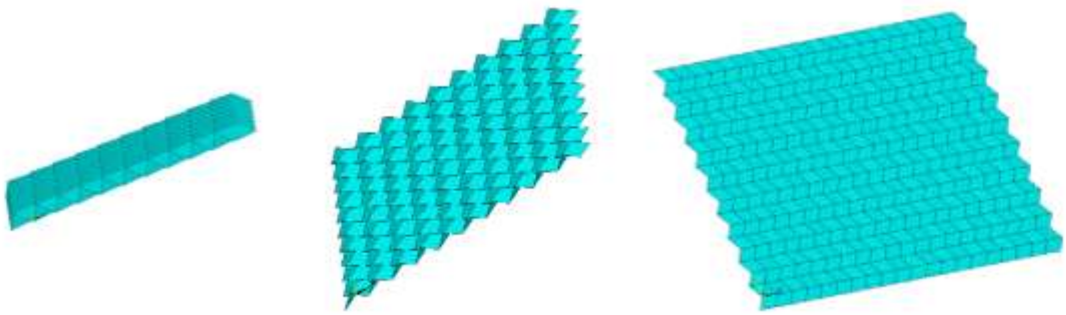

Figure 2. Miura-Ori Origami from folding to unfolding position

It is important to point out that unlike traditional materials, in the case of origami-like materials/structures the planar response of Miura-Ori configuration is categorized by the Poisson's ratio and the stretching rigidity. Both quantities are function of dihedral and oblique angles (θ and α). Moreover, they are constantly changing during the folding/unfolding process. As commented by Wong and Pellegrino (2006), the Poisson's ratio variation during the folding/unfolding process is the main reason for the wrinkles existence in such membranes.

Table 1. Miura-Ori unit cell nodal components

Node ID	X-Coordinate	Y-Coordinate	Z-Coordinate
1	$2\sqrt{(l_1^2 - h^2)}$	0.0	0.0
2	$\sqrt{(l_1^2 - h^2)}$	0.0	0.0
3	0.0	0.0	0.0
4	$2\sqrt{(l_1^2 - h^2)} - \sqrt{\left(l_2^2 - \frac{w^2}{4}\right)}$	$\frac{w}{2}$	0.0
5	$2\sqrt{(l_1^2 - h^2)} - \sqrt{\left(l_2^2 - \frac{w^2}{4}\right)} - \frac{l}{2}$	$\frac{w}{2}$	$\sqrt{\left(l_1^2 - \frac{l^2}{4}\right)}$
6	$2\sqrt{(l_1^2 - h^2)} - \sqrt{\left(l_2^2 - \frac{w^2}{4}\right)} - l$	$\frac{w}{2}$	0.0
7	$2\sqrt{(l_1^2 - h^2)} - \sqrt{\left(l_2^2 - \frac{w^2}{4}\right)}$	$-\frac{w}{2}$	0.0
8	$2\sqrt{(l_1^2 - h^2)} - \sqrt{\left(l_2^2 - \frac{w^2}{4}\right)} - \frac{l}{2}$	$-\frac{w}{2}$	$\sqrt{\left(l_1^2 - \frac{l^2}{4}\right)}$
9	$2\sqrt{(l_1^2 - h^2)} - \sqrt{\left(l_2^2 - \frac{w^2}{4}\right)} - l$	$-\frac{w}{2}$	0.0

Considering the unit cell approach, Wei et al (2013) defined the in-plane Poisson's ratio and the stretching rigidity by the following equations:

Proceedings of the XXXVIII Iberian Latin-American Congress on Computational Methods in Engineering
P.O. Faria, R.H. Lopez, L.F.F. Miguel, W.J.S. Gomes, M. Noronha (Editores), ABMEC, Florianópolis, SC, Brazil, November 5-8, 2017.

$$\boldsymbol{\nu_{wl}} = -\frac{dw/w}{dl/l} = \mathbf{1} - \left(\frac{1}{\xi^2}\right) \tag{7}$$

$$\boldsymbol{\kappa_x} = \frac{4k\left[\left(1-\xi_0^2\right)^2 + cos^2\alpha\right]}{\left(1-\xi_0^2\right)^{0.5} cos\alpha sin^2\alpha sin\theta_0} \tag{8}$$

where θ_0 is the dihedral angle in the undeformed state, and k is the hinge spring constant, which is defined by:

$$\boldsymbol{k} = \frac{EI}{l} \tag{9}$$

From the theory of elasticity discussed in Ávila et al (2011) and based on unit cell described, it is possible to notice two important conditions:

$$\boldsymbol{\xi} \leq \mathbf{1} \tag{10}$$

$$\boldsymbol{\nu_{wl}} < \mathbf{0} \tag{11}$$

The negative in-plane Poisson's seems to be unrealistic, but the Miura-Ori can be considered an auxetic configuration. This condition agrees with the model described in Ishida et al (2017). The Miura-Ori configuration is mostly used into the space technology sector for solar panels, which has the final shape of a flat surfaces. For different space structures, e.g. space telescopes, are designed, a different origami pattern must be employed.

Wilson et al (2013) proposed an origami sunshield concept for space telescope based on Kresling pattern. In this case, the origami structure resembles a tubular bellow. According to Cai et al (2015), the Kresling pattern can support the post-buckling and torsional loadings commonly present during the deploying process of cylindrical structures. Again, the concept of unit cell can be applied. Figure 3 shows a unit cell for the Kresling bellow origami cylindrical structure.

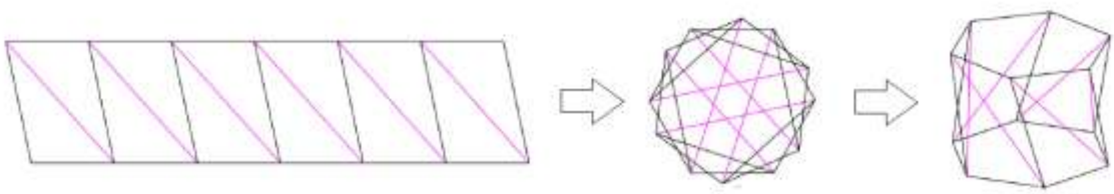

Figure 3. Unit cell construction for Kresling origami pattern from Cai et al (2015)

Cai et al (2015) suggested that the only three variables are to be needed, i.e. the number of edges (n), the unit cell height (h) and the edge size (l). However, if these variables are considered fixed, it will not possible to fold and unfold the Kresling origami. Note that unit cell height (*h*) and radius (*r)* change during the folding/unfolding process. To solve this problem an alternative set of equations based on the unit cell geometry was proposed.

$$\boldsymbol{\varphi} = \frac{\pi}{n} \tag{11}$$

$$\boldsymbol{\beta} = \frac{2\pi}{n} \tag{12}$$

$$\boldsymbol{h} = \frac{l\tan\delta}{\sin\varphi} \tag{13}$$

$$\boldsymbol{r} = \frac{l}{2\sin\varphi} \tag{14}$$

$$\boldsymbol{\theta} = \boldsymbol{\beta} + \frac{h}{2r\tan\delta} \tag{15}$$

where φ is the angle between the edge and the rectangle diagonal, β is polygon angle based on the number of edges, *r* is the outside circle radius, θ is the unit cell rotation angle from one unit cell to another, and δ is the folding angle. Note that the unit cell origin is located at the cylinder center line and at the bottom at the first unit cell. Therefore, by using a Cartesian coordinate system with this origin the unit cell X and Y coordinates are based on projections of cylinder radius. Figure 4 shows different stage from the Kresling origami bellow from near fully folded to near fully unfolded.

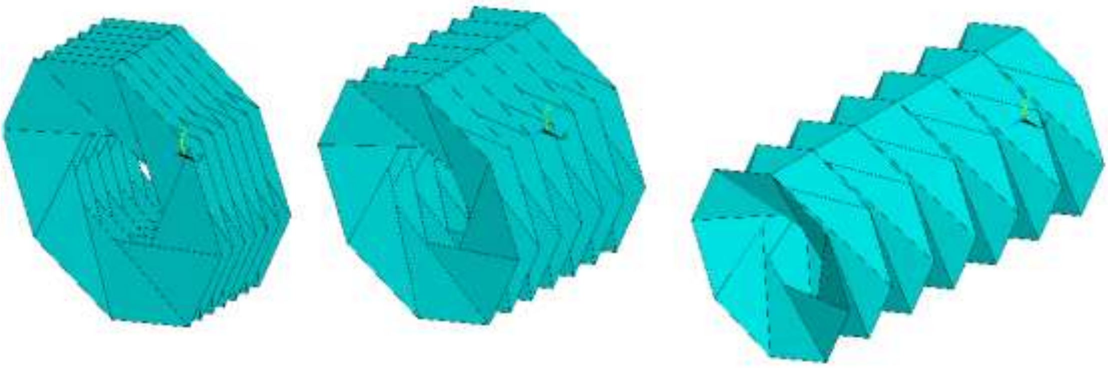

Figure 4. Kresling origami from folding to unfolding positions

The Kresling configuration has the in-plane Poisson's ration defined as:

$$\boldsymbol{\nu}_{hr} = -\frac{dh/h}{dr/r} \tag{16}$$

Proceedings of the XXXVIII Iberian Latin-American Congress on Computational Methods in Engineering
P.O. Faria, R.H. Lopez, L.F.F. Miguel, W.J.S. Gomes, M. Noronha (Editores), ABMEC, Florianópolis, SC, Brazil, November 5-8, 2017.

Contrary to the Miura-Ori Tessellation origami pattern, the Kresling origami has a positive in-plane Poisson's ratio. However, the Poisson's ratio is still variable during the folding/unfolding processes. These variations on Poisson's ratio can cause variations on natural frequencies and bring problems during unfold/deployment operations

EXPERIMETAL PROCEDURES AND NUMERICAL ANALYSIS

To be able to investigate the crease and wrinkle effects into origami-structures behavior let's divide the analysis in two different approaches. The first approach investigates the crease effect into the mechanical properties of thin membranes. To achieve this goal a series of tensile tests following the ASTM D882 (2012) standard was performed. The membrane is made of cellulose acetate with thickness of 100 μm. At least five sample (250 mm x 25 mm) were tested at constant speed of 50 mm/min. To be able to analyze the crease effect into the overall mechanical behavior a 1.0 mm thick crease was made at center section of each sample. Five different groups were analyzed, i.e. the CTRL group (control) was defined as the one without any crease, the 00 group had a center crease at zero deg (longitudinal axis), the 30 group had the crease at 30 deg measured from the longitudinal axis, the 60 groups had creases with 60 deg slope and the 90 group had the creases aligned with the transverse axis. The second approach is based on modal analysis employing the finite element method. As we are dealing with thin membranes, a first order shell element was employed.

DATA ANALYSIS

Figure 5 shows the representative stress-strain curves for the cellulose acetate samples. The stiffness seems not be affected by the crease. The same behavior can be observed for the ultimate strength. The strain at failure, however, suffered significant changes due to the crease location and angular position. This fact seems to be directly related to the failure modes due to off-axis crease locations. Table 2 summarizes the key values obtained during the tensile tests.

The Levene's test of variance for stiffness and strength indicate that populations are not significantly different Unlikely, the Kapton membranes employed by Papa and Pellegrino (2008), the cellulose acetate membrane is only linear in a small portion, up to 0.025 mm/mm. This non-linear behavior can also be another factor to influence the origami –like structure behavior. Nonetheless, it is not clear how the creases will affect the origami overall behavior during the fold/unfold process.

Table 2. Summary of tensile tests

Group ID	Stiffness [MPa]	Strength [MPa]	Strain at Failure [mm/mm]
Control	3408.12±212.99	117.11±8.75	0.66±0.23
0 deg	3166.09±100.75	120.01±4.55	0.84±0.07
30 deg	3948.86±297.77	121.39±16.78	0.61±0.32
60 deg	3841.55±186.46	108.75±11.16	0.34±0.28
90 deg	3656.94±164.32	124.31±5.53	0.85±0.09

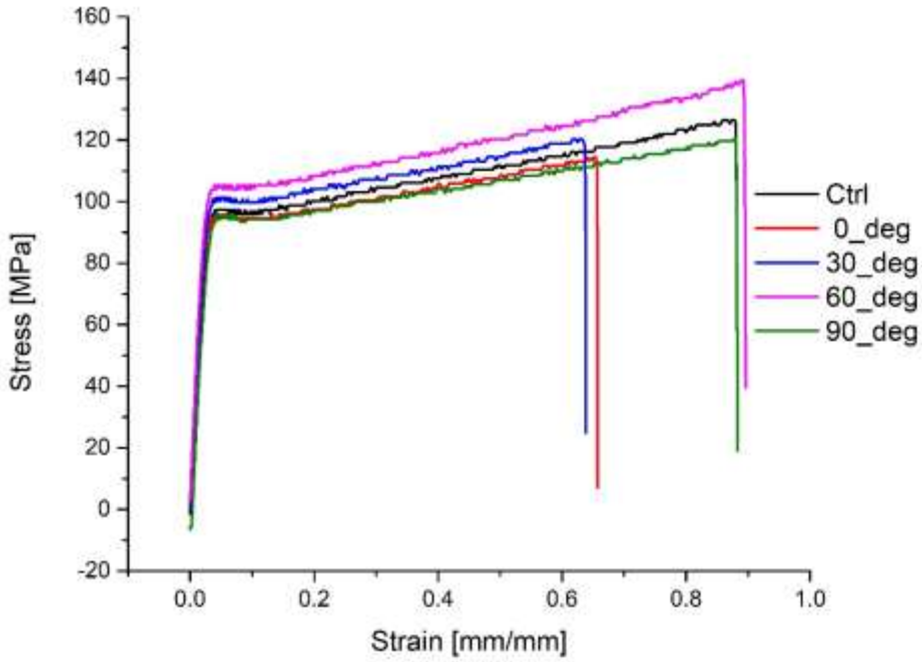

Figure 5. Representative Stress-strain curves for tensile tests

The second type of analysis is to investigate how the Miura-Ori structure overall in-Plane Poisson's ratio behaves during the folding/unfolding process. As it can be observed in Figure 6, the in-plane Poisson's ratio is negative and the large negative is in fact a point of singularity. As commented by Wei et al (2013), so that the two orthogonal planar directions may be folded or unfolded independently, as in traditional map folding. Indeed, this is the unique state for which nonparallel folds are independent, and it might surprise the reader that, with few exceptions, this is the way maps are folded—makes unfolding easy, but folding almost impossible. The results obtained are in good agreement with Wei et al (2013). The stretching rigidity on x direction (Figure 7) has a singularity at $\theta \approx 180$ deg and $\alpha \approx 90$, which corresponding an almost flat condition. It is worth to point out, that Miura-Ori structures have an unique response due to its particular geometry. The in-plane Poisson's ratio for the Kresling pattern follows a monotonic function which is similar to traditional elastic materials, and it will not be discussed in this paper.

The key issue is to evaluate how creases will affect the Miura-Ori and the Kresling patterns. To be able to achieve such goal a modal analysis based on finite element method is performed. The boundary conditions considered are the clamped-clamped one. As discussed by Papa and Pellegrino (2008) solar sail membranes after deployment are fixed/clamped. In the case of telescopes, the clamped-clamped condition can be employed as discussed by Wilson et al (2013).

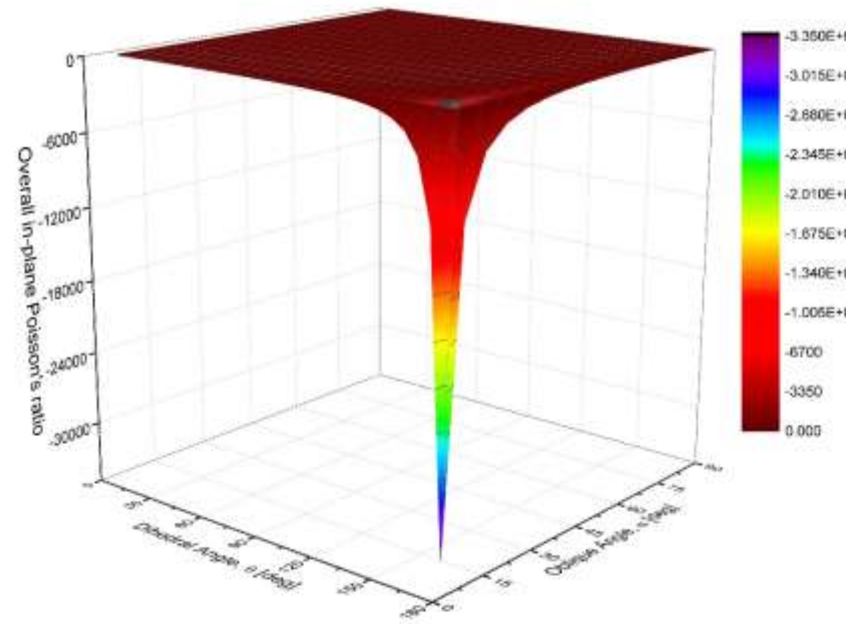

Figure 6. Miura-Ori in-plane Poisson's ratio during deployment

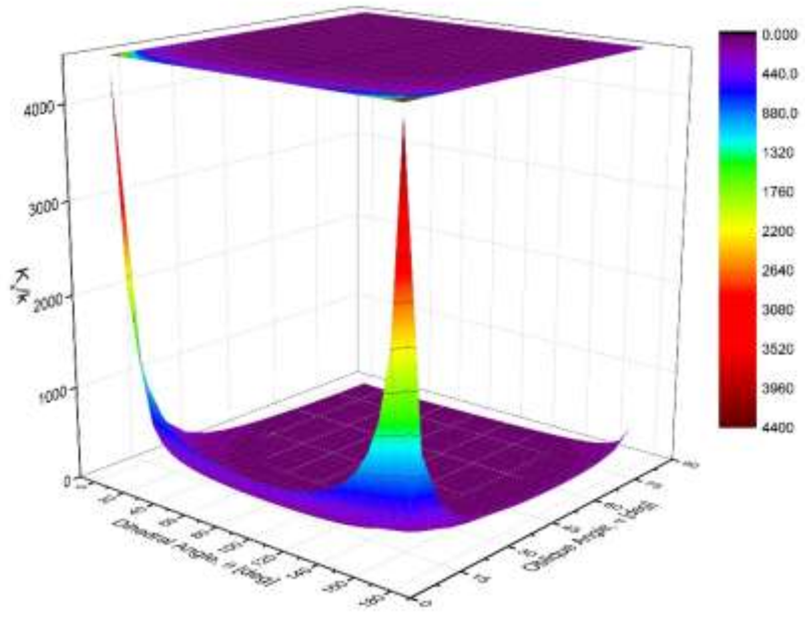

Figure 7. Miura-Ori Stretching rigidity at x direction during deployment

The Miura-ori configuration will be simulated considering a one square meter of area and a thickness of 0.1 mm. The membrane material is cellulose acetate with density of 1.28 g/cm^3. The element employed during simulations are four-node first-order shell elements with 6 degree-of-freedom per node. The oblique angle varies from 15 to 90 deg and the dihedral angle is equal to 67.5 deg. According to Fang et al (2017), the dihedral angle around 67.7 deg defines a stability region. As it can be observed into Figure 8, the increase on creases number affect the natural frequencies. However, it seems that there is a saturation limit in which natural frequencies reach an asymptotic value, but the 45 and 90 deg cases. This phenomenon can be explained by the Poisson's ratio singularity point at the 90 deg condition and the geometric condition at 45 deg, which can introduce additional loss of stiffness. The oblique angle also has an indirect effect the natural frequencies. The combination of dihedral and oblique angles lead to different Poisson's ratio. The Poisson's effect associated to the overall geometry produced different vibration modes. For the α=60 deg, the vibration mode at natural frequency is a combination of torsion and bending, while for α=30 deg, the vibration mode is basically from torsion mode, see Figures 9A and 9B. This can explain the difference on natural frequencies obtained.

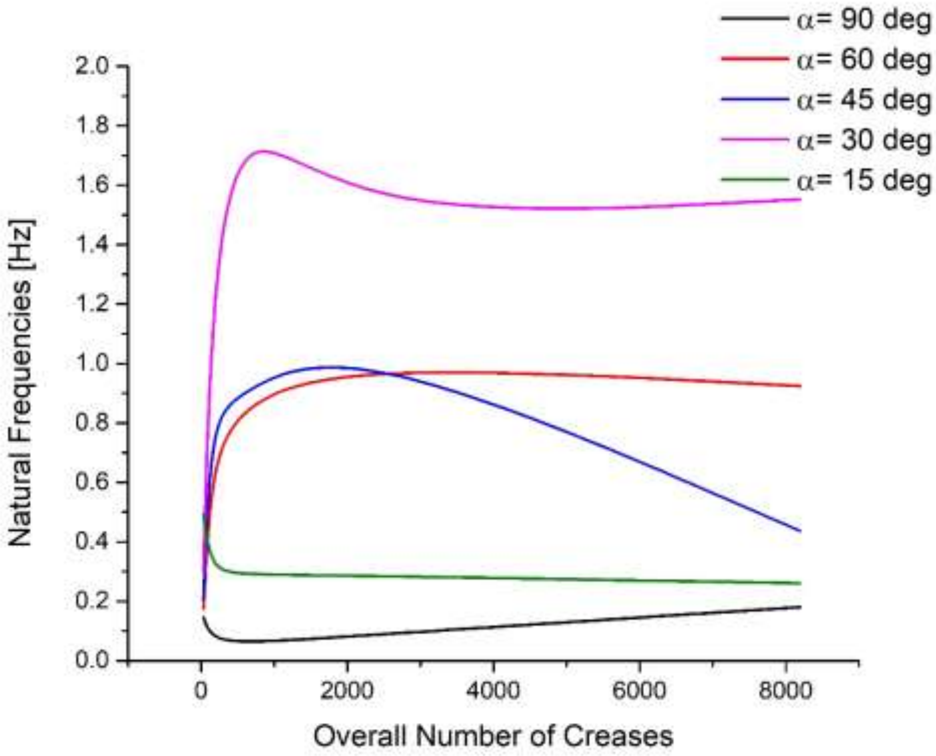

Figure 8. Crease effect into natural frequencies

The last part of the analysis section is related to Kresling pattern. The first phase of this analysis is to understand how the number of creases affects the natural frequencies. In this particular case, the number of creases is proportional to the number of edges at bases. From practical point of view, the number of edges at base cannot increase indefinitely. Hence, the analysis will focus on the most common ones described by Pellegrino (2001), i.e. from 6 to 24 edges. Figure 10 shows the natural frequency variation during three different stages of deployment process, i.e. at δ=5 deg (folding), δ=15 deg (intermediate), and δ=30 deg (deployed).

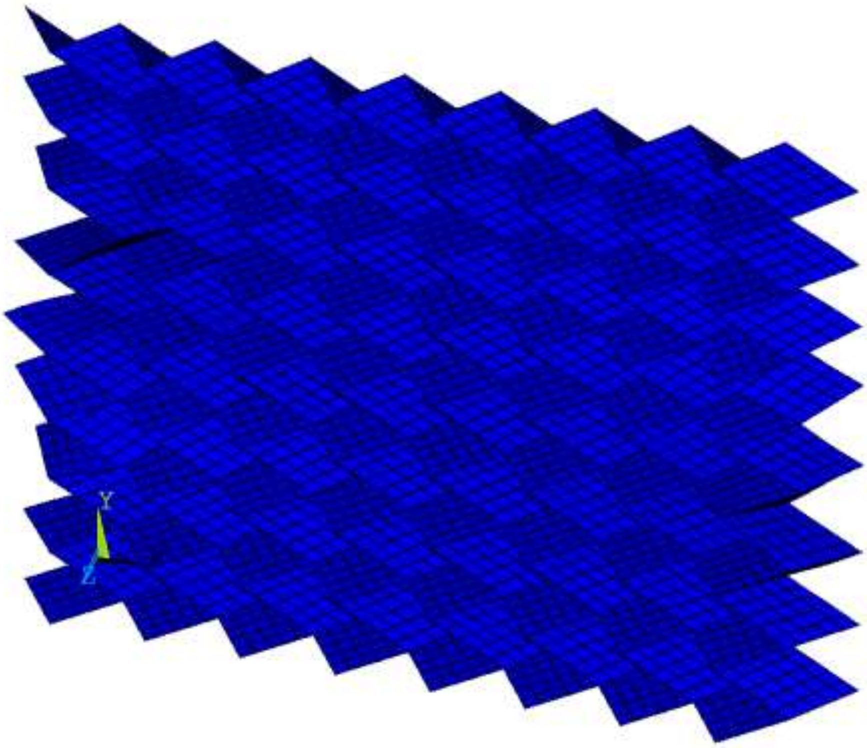

(a)

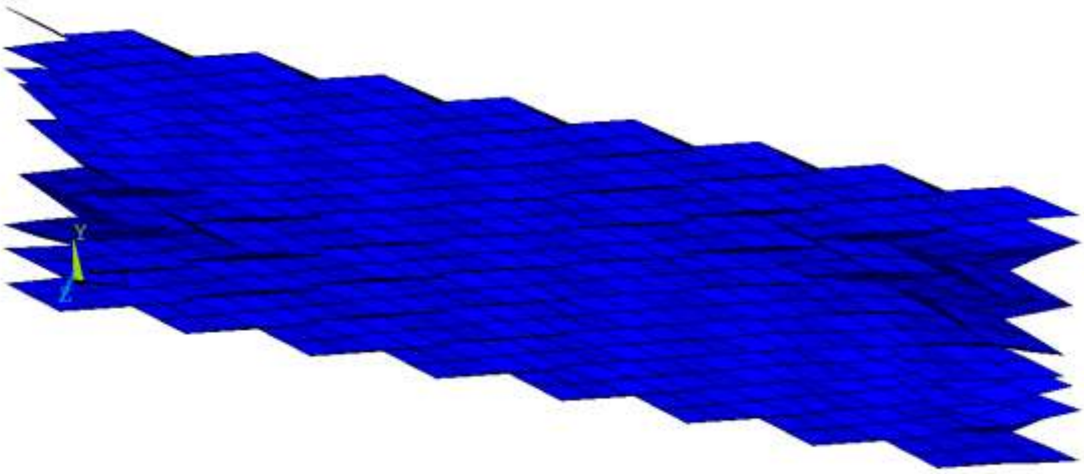

(b)

Figure 9. Vibration mode. (a) α=60 deg, (b) α=30 deg.

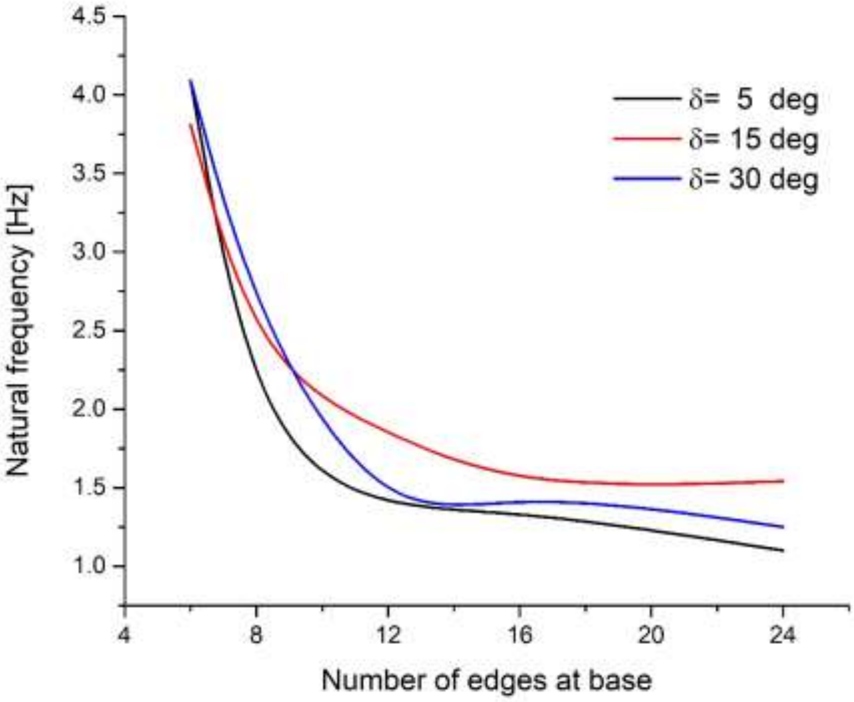

Figure 10. Natural frequency for Kresling origami during the unfolding/deployment

The natural frequencies decreases during the deployment process. Furthermore as the number of creases increases (number of edges at base also increases) the effect on natural frequencies is even more noticeable. Another important issue is the vibration mode at each instant of unfolding process. It can observed in Figures 11-13 during the unfolding process the vibration modes changes. At initial stage of unfolding, the Kresling origami vibrates at Y-Z pane as expected for a below-like structure. (see Fig. 11) As the unfolding/deployment process continued, the aspect ratio base/height increase and at δ=15 deg, the Y-Z vibration is combined with a torsion at Y-X plane, as shown in Figure 12. At near full deployment, i.e. δ=30 deg, the Y-Z plane vibration is not noticeable and the torsion on Y-X plane is predominant. It is important to mention that during deployment buckling can occur. This buckling effect combined with the Kresling pattern geometry could be the cause of such torsion generated during the unfolding process.

This analysis shows two new aspects on origami-like structures, i.e. the first one is the asymptotic behavior of natural frequencies with the increase on crease number for both Miura-Ori and Kresling origami-like structures. The second information is based on mode vibrations changes during the unfolding process, which it is also a critical during space structures deployment. The final feature is the fact that stiffness and strength are independent of the crease orientation for acetate membranes. Yet the non-linear stress-strain behavior is another issue to be taken into consideration for further analysis.

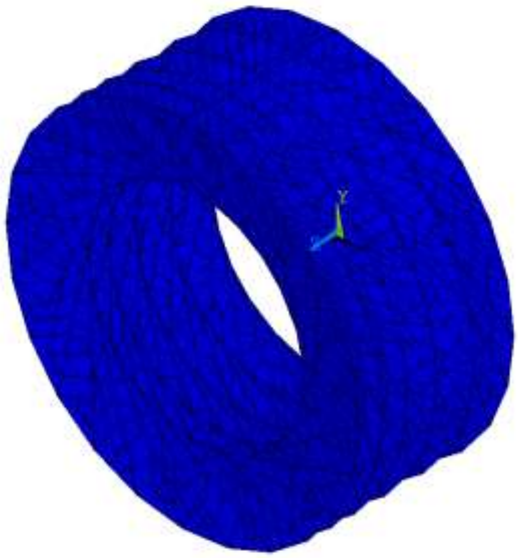

Figure 11. Vibration mode for Kresling origami structures during initial unfolding

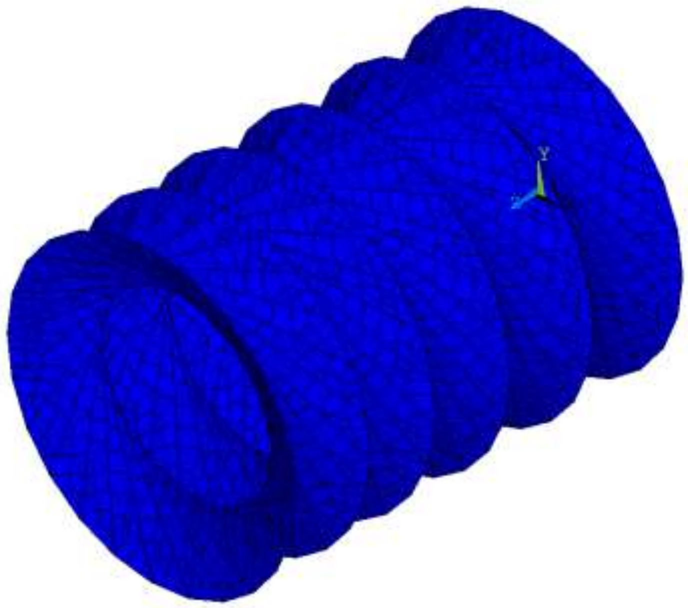

Figure 12. Vibration mode for Kresling origami structures during intermediate unfolding

Proceedings of the XXXVIII Iberian Latin-American Congress on Computational Methods in Engineering
P.O. Faria, R.H. Lopez, L.F.F. Miguel, W.J.S. Gomes, M. Noronha (Editores), ABMEC, Florianópolis, SC, Brazil, November 5-8, 2017.

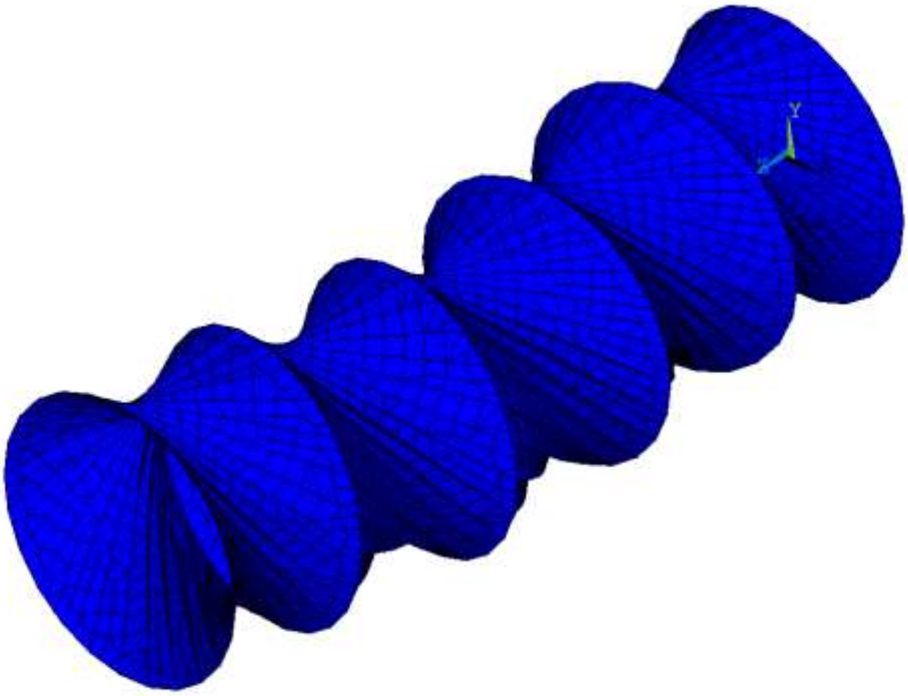

Figure 13. Vibration mode for Kresling origami structures near fully unfolded

CONCLUSIONS

The origami-like structure natural frequencies were studied using modal analysis based on finite element. This analysis shows two new aspects on origami-like structures, i.e. the first one is the asymptotic behavior of natural frequencies with the increase on crease number for both Miura-Ori and Kresling origami-like structures. The second information is based on mode vibrations changes during the unfolding process, which it is also a critical during space structures deployment. The final feature is the fact that stiffness and strength are independent of the crease orientation for acetate membranes. Yet the non-linear stress-strain behavior is another issue to be taken into consideration for further analysis.

ACKNOWLEDGEMENTS

The authors would like to acknowledge the financial support provided by The Air Force Office of Scientific Research (AFOSR) under grant FA9550-14-1-0377 and the Brazilian Research Council under grant 304646/2014-8.

REFERENCES

ASTM D 880, 2012. Standard Test Method for Tensile Properties of Thin Plastic Sheeting. ASTM *Annual Book of Standards,* vol. 15. n. 3, pp.1-12.

Avila, A.F., Eduardo, A.C., & Silva Neto, A., 2011. Vibration analysis of graphene based nanostructures, *Computers and Structures*, vol. 89, n. 4, pp.878-892.

Cai, J., Xiaowei, D., Ya, Z., Jian, F., & Yongming, T. 2015. Bistable behavior of the cylindrical origami structure with Kresling pattern. *Journal of Mechanical Design,* vol. 137, n. 5, pp.061406-8.

Cai, J., Ren, Z., Ding, Y., Deng, X., Xu, Y., & Feng, J. 2017. Deployment simulation of foldable origami membrane structures. *Aerospace Science and Technology,* vol. 67, n. 2, pp. 343-353.

Chen, Y., & Feng, J., 2012. Folding pf a type of deployable origami structures. *International Journal of Structural Stability and Dynamics,* vol. 12, n. 6, pp.1250054-17.

Dutta, S., & Graham, M.D., 2017. Dynamics of Miura-patterned foldable sheets in shear flow. *Soft Matter,* vol. 13, n.12, pp. 2620-2633.

Fang, H., Li, S., Ji, H., & Wang, K.W., 2017. Dynamics of a bistable Miura-origami structure. *Physical Review,* vol. 95, n.12, pp. 052211-11.

Ishida, S., Uchida, H., Shimosaka, H., & Hagiwara, I. 2017. Design and numerical analysis of vibration isolators with quasi-zero-stiffness characteristics using bistable foldable structures. *Journal of Vibration and Acoustics,* vol. 139, n. 3, pp.031015-8.

Liu, S., Lu, G., Chen, Y., & Leng, Y.W., 2015. Deformation of the Miura-Ori patterned sheet. *International Journal of Mechanical Sciences,* vol. 99, n. 1, pp.130-142.

Papa, A., & Pellegrino, S. 2008. Systematically creased thin-film membrane structures. *Journal of Spacecraft and Rockets,* vol. 45, n. 1, pp. 10-18.

Pellegrino, S., 2001. Deployable Structures in Engineering. In *Deployable Structures*, Sergio Pellegrino (ed.), Springer, pp.1-35.

Wang, F., Gong, H., Chen, X., & Chen, C.Q., 2016. Folding to curve surfaces: A generalized design method and mechanics of origami-based cylindrical structures. *Scientific Reports,* vol. 6, pp. 33312-10.

Wang, C.-G., Tan, H.-F., & He, X.-D. 2011. Wrinkle-crease interaction behavior simulation of rectangular membrane under shearing. *Acta Mechanica Sinica,* vol. 27, n.4, pp. 550-558.

Wei, Z.Y., Guo, Z.V., Dudte, L., Liang, H.Y., & Mahadevan, L. 2013. Geometric mechanics of periodic pleated origami. *Physical Review Letters,* vol.110, n.5, pp. 215501-5.

Wilson, L, Pellegrino, S., & Danner, R. 2013. Origami sunshield concepts for space telescopes. *Proceedings of the 54th AIAA/ASME/ASCE/AHS/ASC Structures, Structural Dynamics, and Materials Conference, pp. 1-12.*

Wong, Y.W., & Pellegrino, S. 2006. Wrinkled membranes Part II: Analytical Models. *Journal of Mechanics of Materials and Structures,* vol. 1, n.1, pp.25-59.

Woo, K. 2008. Effective modulus of creased thin membranes. *Journal of Spacecraft and Rockets*, vol. 45, n. 1, pp. 19-26.

Yasuda, H., & Yang, J. 2015. Reentrant origami-based metamaterials with negative Poisson's ratio and bistability. *Physical Review Letters,* vol. 114, n. 6, pp.185502-5.

Zhou, X., Zang, S., & You, Z., 2016. Origami mechanical metamaterials based on the Miura-derivative fold patterns. *Proceedings of the Royal Society A,* vol. 472, n.1, pp.361-376.